ELSEVIER

Journal of Biomechanics 40 (2007) 1423–1432

JOURNAL OF BIOMECHANICS

www.elsevier.com/locate/jbiomech
www.JBiomech.com

Sloped muscle excitation waveforms improve the accuracy of forward dynamic simulations

M.J. Camilleri[a], M.L. Hull[a,b,*], Nils Hakansson[a]

[a]*Biomedical Engineering Program, One Shields Avenue, University of California, Davis, CA 95616, USA*
[b]*Department of Mechanical Engineering, One Shields Avenue, University of California, Davis, CA 95616, USA*

Accepted 12 June 2006

Abstract

Mathematical models of the muscle excitation are useful in forward dynamic simulations of human movement tasks. One objective was to demonstrate that sloped as opposed to rectangular excitation waveforms improve the accuracy of forward dynamic simulations. A second objective was to demonstrate the differences in simulated muscle forces using sloped versus rectangular waveforms. To fulfill these objectives, surface EMG signals from the triceps brachii and elbow joint angle were recorded and the intersegmental moment of the elbow joint was computed from 14 subjects who performed two cyclic elbow extension experiments at 200 and 300 deg/s. Additionally, the surface EMG signals from the leg musculature, joint angles, and pedal forces were recorded and joint intersegmental moments were computed during a more complex pedaling task (90 rpm at 250 W). Using forward dynamic simulations, four optimizations were performed in which the experimental intersegmental moment was tracked for the elbow extension tasks and four optimizations were performed in which the experimental pedal angle, pedal forces, and joint intersegmental moments were tracked for the pedaling task. In these optimizations the three parameters (onset and offset time, and peak excitation) defining the sloped (triangular, quadratic, and Hanning) and rectangular excitation waveforms were varied to minimize the difference between the simulated and experimentally tracked quantities. For the elbow extension task, the intersegmental elbow moment root mean squared error, onset timing error, and offset timing error were less from simulations using a sloped excitation waveform compared to a rectangular excitation waveform ($p<0.001$). The average and peak muscle forces were from 7% to 16% larger and 20–28% larger, respectively, when using a rectangular excitation waveform. The tracking error for pedaling also decreased when using a sloped excitation waveform, with the quadratic waveform generating the smallest tracking errors for both tasks. These results support the use of sloped over rectangular excitation waveforms to establish greater confidence in the results of forward dynamic simulations.

Keywords: Forward dynamic; Simulation; Excitation waveform; Force; Optimization; Tracking problem; Elbow extension; Muscle; Recumbent pedaling

1. Introduction

Forward dynamic simulations of human movement tasks provide valuable knowledge related to the neuromuscular strategies of performing these tasks. These simulations implement neuro-musculo-skeletal models to simulate task kinematics and kinetics and either solve an open-ended problem (goal-directed prediction of the kinematics and kinetics of a task) or solve a ''tracking-problem'' (replication of the kinematics and kinetics of a task). Returned by the simulations is quantitative information regarding joint torques and muscle forces, as well as excitation timing and activation of individual muscles. Simulation results may be used for purposes such as optimizing a task (Bobbert and van Zandwijk, 1999), understanding principles of motor control (Raasch et al., 1997; Neptune and Hull, 1998), and

*Corresponding author. Department of Mechanical Engineering, One Shields Avenue, University of California, Davis, CA 95616, USA. Tel.: +1 530 752 6220; fax: +1 530 752 4158.
E-mail address: mlhull@ucdavis.edu (M.L. Hull).

0021-9290/$ - see front matter © 2006 Elsevier Ltd. All rights reserved.
doi:10.1016/j.jbiomech.2006.06.009

minimizing the risk of injury during rehabilitation (Li et al., 1998). Whether either simulating an open-ended problem or solving a tracking-problem, the models (neural, muscular, and skeletal) used must be accurate for the simulations to return meaningful results.

The first model which is implemented in a forward dynamic simulation is the waveform that represents the neural excitation signals that stimulate the muscles. These neural excitation waveforms are generally transformed into muscle activations which in turn are transformed into muscle forces that act on the body segments to generate intersegmental loads (Zajac, 1989). Because the neural excitation waveform is the input to the remaining processes which must be modeled in a forward dynamic simulation, any inaccuracy in this excitation waveform will propagate through the entire simulation. Therefore generating improved excitation waveforms is a subject of high interest.

An ideal excitation waveform would (1) generate accurate results, (2) be defined by verifiable parameters, (3) be widely applicable, and (4) would require few resources (e.g. time and money) to implement. Unfortunately, no single excitation waveform satisfies all of these criteria. EMG-driven models, which compute the muscle excitation by filtering the EMG signal based on a few parameters, can be calibrated for accuracy using one set of experiments and verified using an additional set of experiments (Lloyd and Besier, 2003). However, EMG-driven models cannot be applied to simulations in which EMG data are not readily available (e.g. simulations involving deep muscles and open-ended simulations) and additional resources for the calibrating experiments are required. Static optimization methods (Anderson and Pandy, 2003; Thelen et al., 2003), which track experimental data at many instances throughout a task, can be applied when EMG data are not available and generate a solution considerably faster than dynamic methods. However, static optimization methods cannot be applied unless experimental data are available and thus cannot be used for open-ended simulations. Additionally, few of the large number of optimized parameters (excitation at each instant) can be independently verified. In contrast, two of the three parameters defining rectangular waveforms can be verified (onset and offset times), and these waveforms can be applied to open-ended simulations (Raasch et al., 1997; Neptune and Hull, 1998). However, the simplicity of rectangular waveforms may result in decreased accuracy and their use increases computational time compared to static optimization methods because they are used within dynamic optimizations.

Because of the limitations in the various excitation waveforms mentioned above, the general aim of this research was to demonstrate the improvement in accuracy of forward dynamic simulations using new excitation waveforms that also largely satisfy the remaining criteria of an ideal waveform. Because large discontinuities in the neural excitation are unlikely and because EMG data suggest that the excitation has a nonzero rise-time to its peak value, we hypothesized that waveforms with a nonzero rise-time to their peak values or a "sloped" waveform (e.g. triangular, quadratic, Hanning) would better replicate the actual excitation and hence improve the accuracy of forward dynamic simulations when compared to a rectangular waveform. Therefore, the first objective of this study was to demonstrate any differences in tracking accuracies between rectangular and sloped waveforms. Because muscle forces are often of interest in simulation studies, a second objective was to demonstrate any differences in average and peak muscle forces using sloped excitation waveforms versus a rectangular excitation waveform.

2. Methods

2.1. First objective

To test the hypothesis that sloped waveforms better replicate the actual excitation compared to rectangular waveforms and hence improve the accuracy of forward dynamic simulations, EMG, kinematic, and kinetic data were collected as fourteen subjects performed cyclic experiments at the elbow joint. The subjects were recruited from the University community and each gave written informed consent. The data acquisition system and experimental apparatus (Fig. 1) consisted of an exercise ergometer, a wrist brace, three surface EMG electrodes, a data acquisition computer with an analog-to-digital converter, and custom data acquisition software written with LabVIEW (National Instruments, Austin, TX). The lateral humeral epicondyle of the subject's elbow on the dominant arm was aligned with the axis of rotation of the ergometer (Cybex 6000, Computer Sports Medicine, Norwood, MA). Dominance was defined as the arm naturally used when

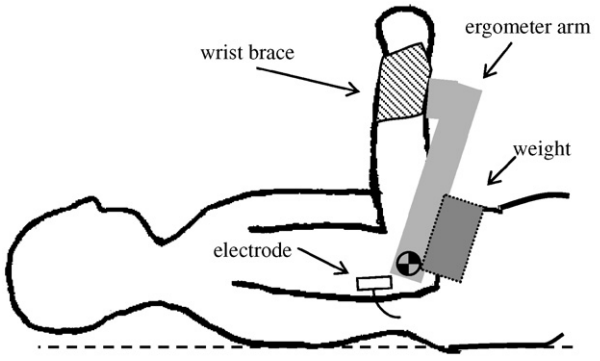

Fig. 1. Diagram of the experimental setup. During elbow flexion the weight, attached to the ergometer arm, provided the net extensive moment that the ergometer required for motion.

turning a wrench. Bipolar surface electrodes (Motion-Lab Systems, Baton Rouge, LA) were placed on the shaved and cleaned skin over the motor endplate (Delagi and Perotto, 1980) of each of the triceps brachii, and the biceps brachii.

The subjects laid supine at the ergometer, with anatomical joint positions controlled prior to the cyclic experiments. The shoulder was at 0° flexion while the wrist was at 0° flexion and the forearm was in the neutral position with respect to pronation/supination. The chest and upper arm were strapped to the ergometer.

The maximum intersegmental elbow moment at 90° elbow flexion was determined prior to performing any data collection (0° flexion = full extension). Three trials of isometric elbow extension were performed at maximum voluntary effort with a minimum of 2 min between trials. The maximum intersegmental elbow moment was defined as the average moment of these three trials.

Each subject performed two dynamic cyclic experiments in which the elbow range of motion was from approximately 10–90° flexion. The ergometer was programmed in "active" mode so that (1) a net extension elbow moment was required for ergometer motion and (2) the absolute value of the maximum ergometer joint angular velocity in both flexion and extension was 200°/s in one experiment and 300°/s in the other experiment. Additionally, the ergometer arm was weighted so that no intersegmental elbow moment was required during elbow flexion (Fig. 1). The average elbow moment during the extensive phase was displayed in real time so that the subjects could target an average intersegmental moment of approximately 0.5 muscle activation as determined by forward dynamic simulations.

To determine whether the simulation accuracy was different between rectangular and sloped waveforms, tracking problems were solved using a rectangular waveform and three sloped waveforms (triangular, quadratic, and Hanning). Data required for these simulations were the experimental and simulated intersegmental elbow moments and angles throughout the flexion-extension cycle.

The experimental intersegmental elbow joint moment (M) was computed by performing inverse dynamic analyses. The equation of motion was generated based on a subject-specific rigid body model using anthropometric data estimated from each subject. The rigid body model consisted of the moment of inertia of the forearm and hand, the forearm-hand mass, and the distance of the center of mass of the forearm-hand to the elbow joint axis. The anthropometric data were estimated using scaling factors (de Leva, 1996). The net elbow joint moment and angular position were sampled at 500 Hz, filtered with a zero-phase-shift second-order Butterworth filter with a low-pass cutoff of 10 Hz, and then averaged across ten cycles. M was computed over the averaged flexion-extension cycle at every 2 ms.

The simulated intersegmental elbow joint moment ($\hat{M}$) was used to track M and its value was computed by performing forward dynamic analyses using each of the four excitation waveforms as inputs to four separate simulations. Each of the four waveforms was defined by three parameters: onset time, offset time, and peak excitation.

$$
\begin{aligned}
&t < t_n \quad \{u = 0\\
&t > t_f \quad \{u = 0\\
&t_n <= t <= t_f \begin{cases} \text{rectangular}: \; u = p, \\ \text{triangular}: \; u = p + \left|t - \frac{t_f + t_n}{2}\right| \left(\frac{-2p}{t_f - t_n}\right), \\ \text{quadratic}: \; u = \frac{-p(t-(t_f+t_n)/2)^2}{((t_f-t_n)/2)^2} + p, \\ \text{Hanning}: \; u = -\frac{p}{2}\cos\left(\frac{t-t_n}{t_f-t_n}2\pi\right) + \frac{p}{2}, \end{cases}
\end{aligned}
\tag{1}
$$

where u is the excitation, t_n is the onset time, t_f the offset time, and p is the peak excitation (Fig. 2). The excitation waveform was passed into a first-order differential equation modeling the activation dynamics (Zajac, 1989), and the resulting activation signal was used as the input into the remainder of the forward simulation model. This model has been detailed elsewhere (Camilleri and Hull, 2005). The force of each of the triceps was computed using a Hill-type equation that required as variable inputs the muscle activation, length, and velocity. The muscle forces were transformed into simulated elbow joint moments by multiplying the forces by the triceps brachii moment arm, the sum of these moments being $\hat{M}$. $\hat{M}$ was determined at each instant in time that the inverse dynamic analyses were performed.

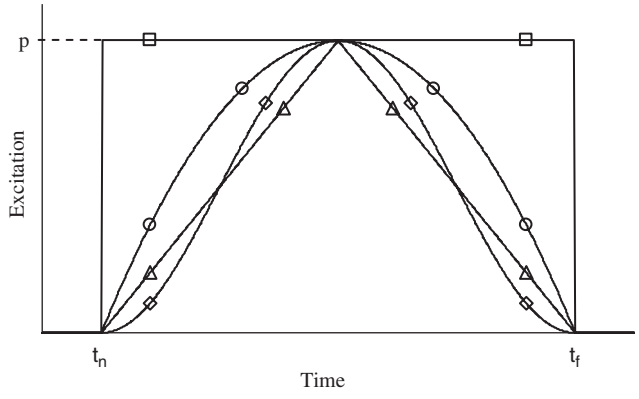

Fig. 2. The four excitation waveforms used in the simulations (□ = rectangular, △ = triangular, ○ = quadratic, ◇ = Hanning). p is the peak excitation, t_n is the onset time, and t_f is the offset time.

The optimized parameter values for each excitation waveform were determined by solving tracking problems. An initial guess of the parameter values was made and the root mean squared error (RMSE) between M and $\hat{M}$ was computed using the following equation:

$$\mathrm{RMSE} = \sqrt{\frac{\sum_{i=1}^{n}(M_i - \hat{M}_i)^2}{n}}, \quad (2)$$

where n is the number of data points. The parameters were varied and optimized by minimizing the RMSE using a simulated annealing algorithm (Goffe et al., 1994). To compare values across subjects, the normalized RMSE was computed by dividing the RMSE by the experimental intersegmental elbow moment averaged across the trial being tracked.

To identify significant differences in the RMSE between the individual waveforms post hoc tests with Bonferonni corrections were performed. Paired t tests for each waveform pair were performed with the level of significance set at $p<0.05/b$, where $b=6$ for the Bonferonni correction, so that the experiment-wise level of significance was 0.05.

Because the muscle onset and offset times were not used as tracking quantities, the errors between the experimental and simulated onset and offset times were used as independent measures of accuracy of the waveforms. The experimental muscle onset and offset times were determined using the EMG data. The EMG data were sampled at 1000 Hz, full-wave rectified, and then low-pass filtered with a zero-phase-shift second-order Butterworth filter with a cutoff of 10 Hz. The data were then resampled at 500 Hz so that the sampling rate was the same as that used in the simulations. The resampled data for each subject were then averaged across 10 cycles. The muscle onset was defined to occur when the EMG activity increased to greater than 3 standard deviations of the baseline EMG activity (Bedingham and Tatton, 1984) that was collected prior to exercising with the elbow at 90° flexion and the musculature at rest. Muscle offset was defined to occur when the EMG activity decreased to below 3 standard deviations of the baseline. To identify significant differences in the onset and offset times between the individual waveforms post hoc tests with Bonferonni corrections were performed. Paired t tests for each waveform pair were performed for both onset and offset times with the level of significance set at $p<0.05/b$, where $b=12$ for the Bonferonni correction, so that the experiment-wise level of significance was 0.05.

To determine whether sloped excitation waveforms provide better tracking accuracies than a rectangular excitation waveform for a relatively complex task, the tracking errors for simulations using rectangular, triangular, quadratic, and Hanning excitation waveforms were computed and compared for a pedaling task. The musculo-skeletal model and optimization routine were similar to that detailed in Neptune and Hull (1998) except that the body was oriented in a recumbent position to reflect the experimental data that were tracked (recumbent pedaling at 90 rpm and 250 W, Hakansson and Hull, 2005). The quantities tracked were the right pedal angle, crank torque, ankle, knee, and hip intersegmental moments, and the horizontal and vertical pedal forces averaged across all subjects.

Pedal angle data and subject limb kinematics were determined using high-resolution video-based motion analysis (Motion Analysis Corp., Santa Rosa, CA). Two spherical reflective markers were placed 30-cm apart in line with the top surface of the pedal and three spherical markers were placed at three fixed points on the ergometer. These two sets of markers were used to develop virtual markers to identify the pedal and crank spindles. Spherical markers were also placed over the anterior superior iliac spine, greater trochanter, lateral epicondyle, and lateral malleolus of the right leg of each subject to capture the limb kinematics. Four high-speed video cameras recorded the three-dimensional marker positions. The three-dimensional marker positions were then projected on the sagittal plane as defined by the path of the pedal spindle. The pedal forces were measured using a two-load component pedal dynamometer (Newmiller et al., 1988). The experimental kinematic and kinetic data recorded as the subjects pedaled the ergometer were used to compute the intersegmental moments using a standard inverse dynamics approach.

The sagittal-plane skeletal model consisted of the pelvis fixed in the ergometer frame with joint motions at the hips, knees, ankles, pedal spindles, and crank spindle. Twenty-eight musculo-tendon complexes were included within nine functional muscle sets. Muscle excitations were passed into a first-order differential equation modeling the activation dynamics (Raasch et al., 1997), and the resulting activation signals were used as the inputs into the remainder of the forward simulation model. Muscle forces were computed using a Hill-type equation that required as variable inputs the muscle activation, length, and velocity. Due to dynamic coupling both the body segments and joints were accelerated by these forces, producing simulated data that were used to track the experimental data. Tracking was performed by minimizing the RMSE of the pedaling quantities normalized to the intersubject standard deviation (NRMSE):

$$\mathrm{NRMSE} = \sqrt{\frac{\sum_{j=1}^{m}\sum_{i=1}^{n}((Y_{ij} - \hat{Y}_{ij})^2/\mathrm{SD}_{ij}^2)}{mn}}, \quad (3)$$

where Y_{ij} is the experimentally measured data, $\hat{Y}_{ij}$ is the model data, n is the number of data points, $m=7$, the number of tracking quantities, and SD_{ij} is the

intersubject standard deviation. The tracking errors (NRMSE) were then compared between simulations from the four excitation waveforms. Similar to the elbow extension task, the errors between the experimental and simulated onset and offset times were used as independent measures of accuracy of the waveforms. Onset and offset timing errors were averaged across the muscles within a simulation and these results were plotted against the waveform to demonstrate any differences.

2.2. Second objective

To demonstrate the differences in elbow extension simulation results when using the four excitation waveforms, both the average and peak muscle forces were determined when using each of the sloped waveforms and the rectangular waveform. The average muscle force was computed over the time that the muscle was active. Two normalization procedures were performed to control for differences in both muscle strength and activation. First, to control for differences in muscle strength, both force quantities were divided by the maximum isometric muscle force. Second, to control for differences in activation, these quotients were then multiplied by the ratio of the average to maximum experimental intersegmental elbow moment; the average was computed over the particular cycle and the maximum was determined from the isometric tests. To identify significant differences in the normalized average and peak muscle forces between the individual waveforms post hoc tests with Bonferonni corrections were performed. Paired t tests for each waveform pair were performed for both the normalized average and peak muscle forces with the level of significance set at $p<0.05/b$, where $b=12$ for the Bonferonni correction, so that the experiment-wise level of significance was 0.05.

To demonstrate the differences in pedaling simulation results when using the four waveforms, both the average and peak muscle forces for each of the muscles were determined when using each of the sloped waveforms and the rectangular waveform. The average muscle force was computed over the time that the muscle was active. A normalization procedure was performed to control for differences in muscle activation between the muscles so as to present averages of the peak muscle forces. Within each muscle the peak muscle forces returned from each simulation were divided by the average from all simulations (thus variation about 1.0). These quotients were then averaged across all muscles within a simulation and then plotted against the waveform to demonstrate any differences. An identical normalization and averaging process was performed for the average muscle force.

3. Results

The interrelationships between the EMG, elbow intersegmental moment, and elbow flexion angle were as expected. EMG activity and the intersegmental moment began to rise near the beginning of extension (Fig. 3), peaked near mid-extension, and fell to zero near the end of extension. All three quantities demonstrated a single phase that lasted approximately half of the cycle.

The pedal forces, pedal angle, and intersegmental moments developed during recumbent pedaling at 90 RPM and 250 W (Fig. 4) were similar to those developed in normal upright pedaling (Neptune and Hull, 1998).

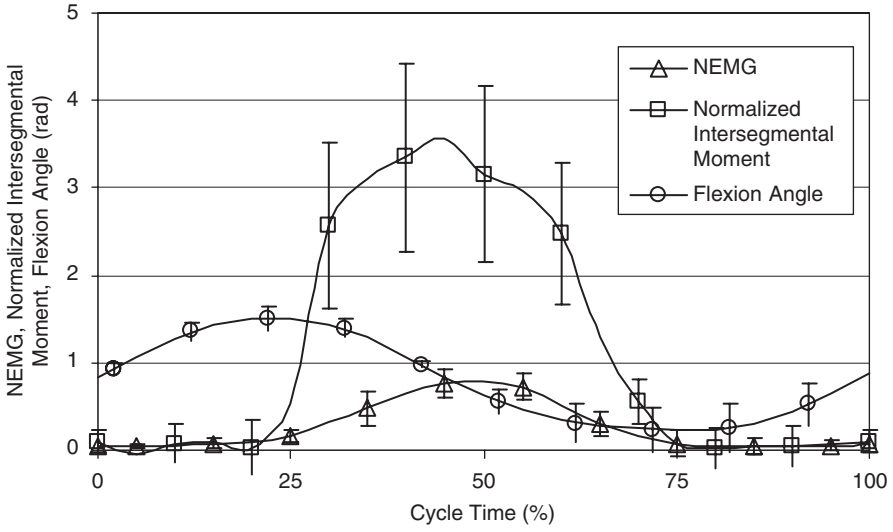

Fig. 3. Experimental elbow data averaged across subjects ($n=14$). The cycle time begins at the midpoint of flexion. NEMG is the EMG normalized to the maximum isometric EMG. The normalized intersegmental moment is normalized to the intersegmental moment averaged across the cycle. The flexion angle is expressed in radians, with full extension at 0 rad.

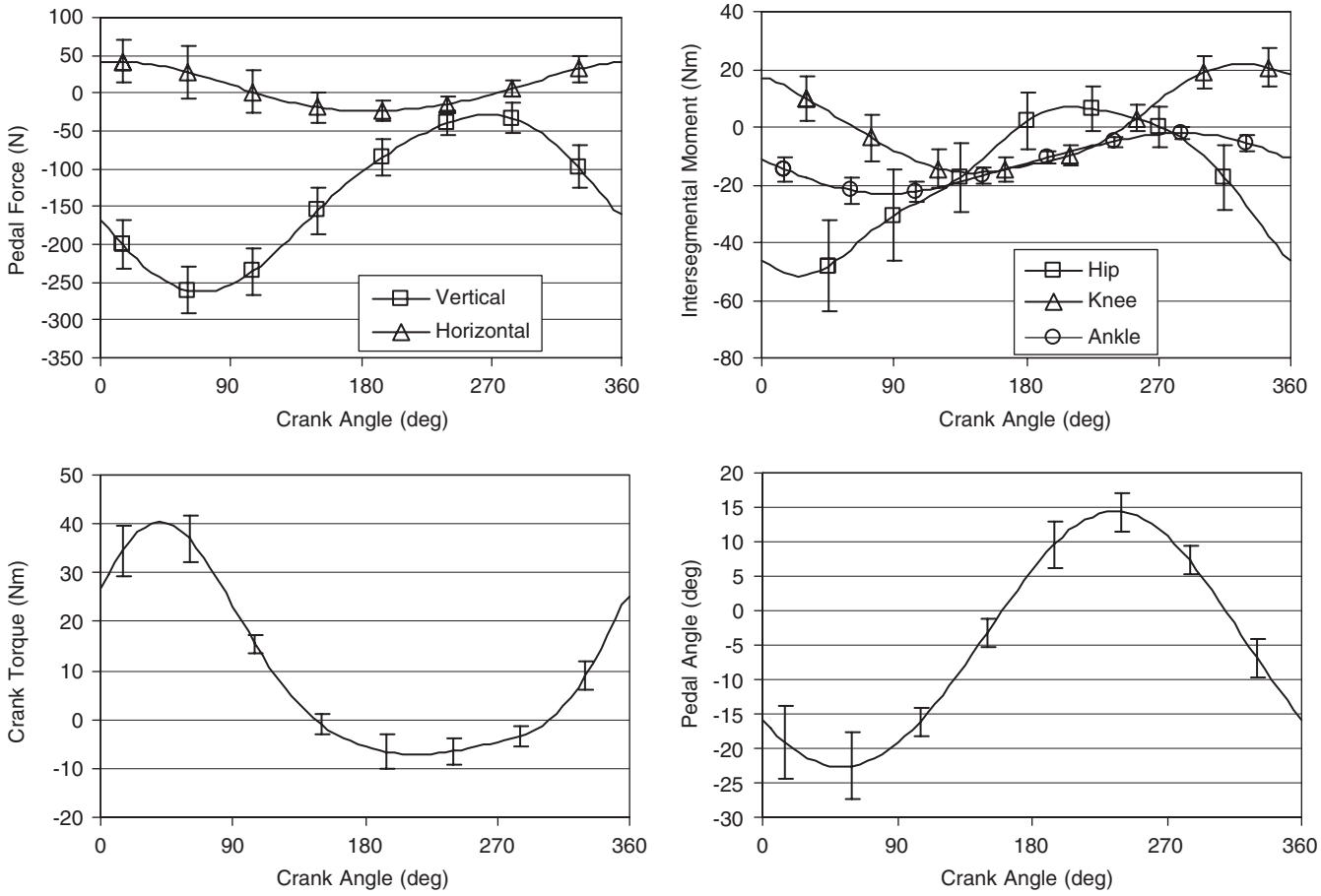

Fig. 4. Experimental pedaling data in the recumbent position averaged across subjects ($n = 15$). A crank angle of 0° is defined when the right crank is oriented 54° counter-clockwise from top-dead center when viewed from the right side. A positive hip intersegmental moment indicates a flexion moment, a positive knee intersegmental moment indicates an extension moment, and a positive ankle intersegmental moment indicates a dorsi-flexion moment.

Additionally, the EMG data demonstrated similar timing between recumbent and normal upright pedaling (Hakansson and Hull, 2005).

3.1. First objective

The simulated elbow extension tasks using different excitation waveforms demonstrated significant differences in both tracking and timing errors ($p<0.001$). Tracking errors were significantly different between all waveform pairs, with the simulations using sloped waveforms demonstrating smaller tracking errors than simulations using rectangular waveforms (Fig. 5). The simulations using the quadratic waveforms had the smallest tracking errors. Both onset and offset errors were significantly different between all waveform pairs ($p<0.001$), with the simulations using sloped waveforms demonstrating smaller timing errors than simulations using rectangular waveforms (Fig. 6). While the simulations using quadratic waveforms demonstrated onset timing with the smallest errors, the simulations using Hanning waveforms demonstrated offset timing with the smallest errors.

The trends of the tracking errors versus waveform for the pedaling task were similar to those of the elbow extension task (Fig. 5). Tracking errors were smaller using sloped waveforms than using the rectangular waveform (from 2 to 15% relative to the rectangular waveform) with the smallest error occurring for the quadratic waveform. Timing errors also were smaller using sloped waveforms (from 29% to 79% relative to the rectangular waveform) (Fig. 7).

3.2. Second objective

For the elbow extension task both the average and peak muscle forces were significantly different for all waveform pairs ($p<0.001$) except one. The peak muscle forces from simulations for the quadratic and triangular waveform pair were not significantly different ($p = 0.0045$). Simulations using rectangular waveforms consistently overestimated these quantities when compared to simulations using sloped waveforms (Fig. 8),

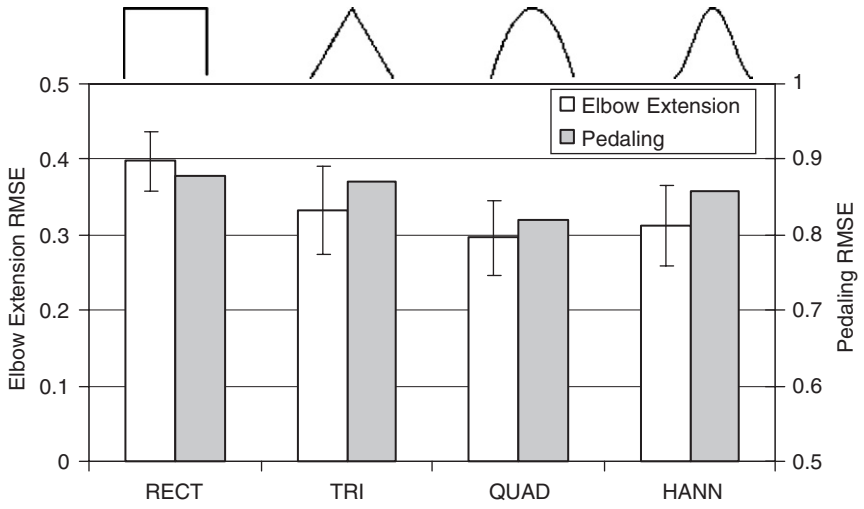

Fig. 5. Normalized RMSEs from the simulations using the four excitation waveforms for both the elbow extension task (unfilled bars) and the pedaling task (filled bars) (RECT = rectangular, TRI = triangular, QUAD = quadratic, HANN = Hanning). For both tasks RMSEs were lower for the sloped waveforms than those for the rectangular waveform. The RMSEs were significantly lower for the elbow extension task ($p<0.001$).

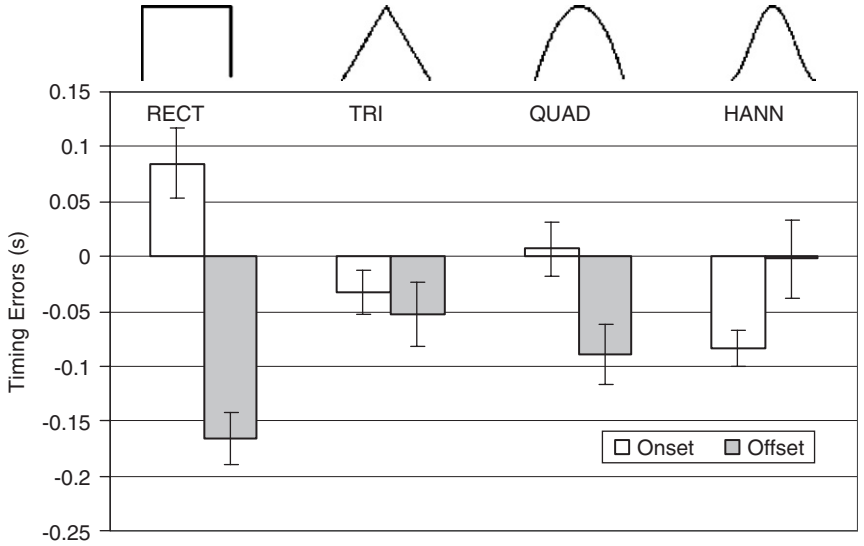

Fig. 6. Onset timing errors (unfilled bars) and offset timing errors (filled bars) from the simulations using the four excitation waveforms for the elbow extension task (RECT = rectangular, TRI = triangular, QUAD = quadratic, HANN = Hanning). Positive values indicate that the simulated timing occurred later than the experimental timing. Errors were significantly lower for the sloped waveforms than those for the rectangular waveform ($p<0.001$).

with the average muscle force overestimated from 7% to 16% and the peak muscle force overestimated from 20% to 28%, relative to the rectangular simulations (Table 1). These quantities were similarly overestimated in the pedaling task using rectangular waveforms, with the average muscle force overestimated from 10% to 21% and the peak muscle force overestimated from 21% to 27%, relative to the rectangular simulations (Fig. 9).

4. Discussion

Although forward dynamic simulation of movement tasks is a powerful technique for providing insight into the muscle control strategies and loading of musculoskeletal structures during these tasks, the excitation waveforms used previously have various limitations. Accordingly, one objective of this study was to test the hypothesis that sloped excitation waveforms with a minimum number of waveform parameters that do not require calibrating experiments better replicate the actual excitation than a rectangular waveform and hence provide more accurate simulation results. A second objective was to compare the differences in the simulation results generated by rectangular and sloped excitation waveforms. An important finding related to the first objective was that the optimized sloped excitation waveforms generate simulation results with

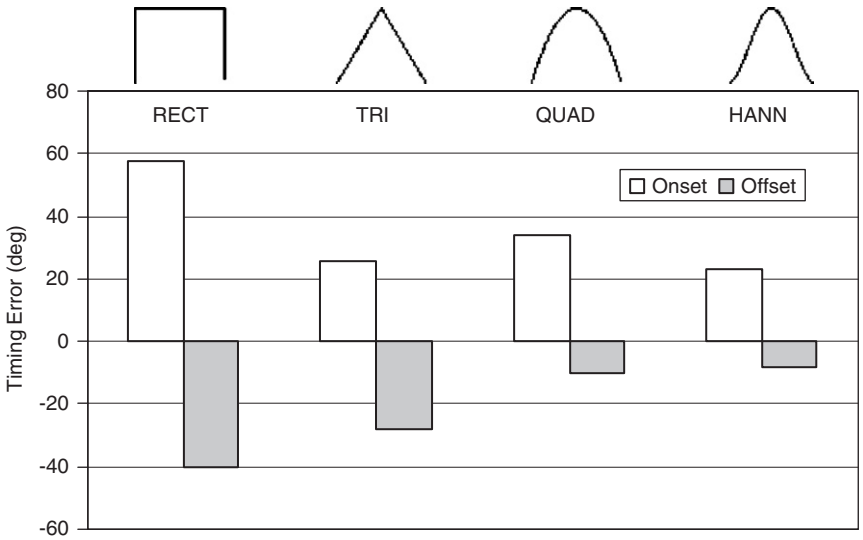

Fig. 7. Average onset timing errors (unfilled bars) and offset timing errors (filled bars) from the simulations using the four excitation waveforms for the pedaling task (RECT = rectangular, TRI = triangular, QUAD = quadratic, HANN = Hanning). Positive values indicate that the simulated timing occurred later than the experimental timing. Timing errors were smaller for sloped waveforms than those for the rectangular waveform.

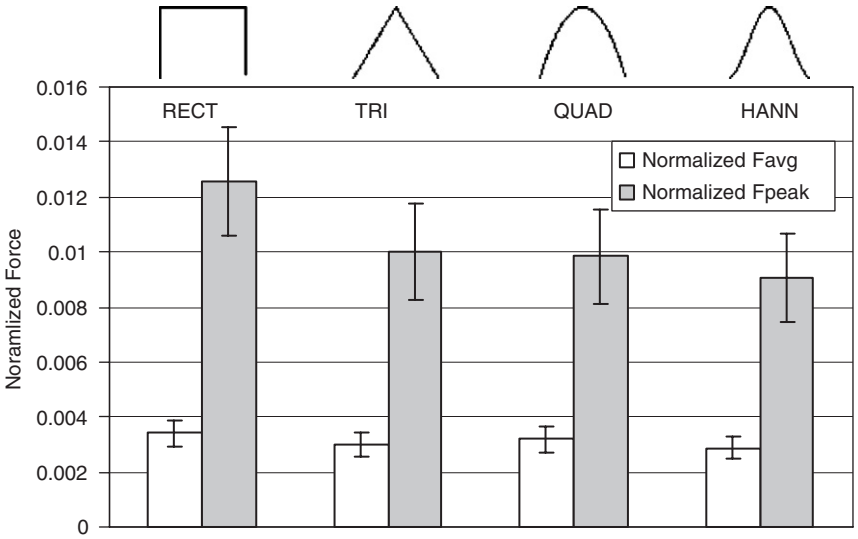

Fig. 8. Normalized average (unfilled bars) and peak (filled bars) muscle forces from the simulations using the four excitation waveforms for the elbow extension task (RECT = rectangular, TRI = triangular, QUAD = quadratic, HANN = Hanning). Sloped waveforms demonstrated significantly smaller forces than those for the rectangular waveform ($p<0.001$).

Table 1
Percent differences in tracking RMSE and simulated force quantities for each of the waveform pairs for the elbow extension task

Waveform pair	Normalized tracking RMSE	Normalized F_{avg}	Normalized F_{peak}
RECT and TRI	16.4	11.9	20.3
RECT and QUAD	25.6	6.9	21.5
RECT and HANN	21.7	16.0	27.9
TRI and QUAD	11.1	−5.6	1.6
TRI and HANN	6.4	4.7	9.5
QUAD and HANN	−5.3	9.8	8.1

RECT = rectangular, TRI = Triangular, QUAD = quadratic, HANN = Hanning.All percentages are expressed as the difference between the first and second waveform normalized to the first waveform in a pair. All pairs were significantly different ($p<0.001$) except for TRI and QUAD for F_{peak} ($p = 0.0045$).

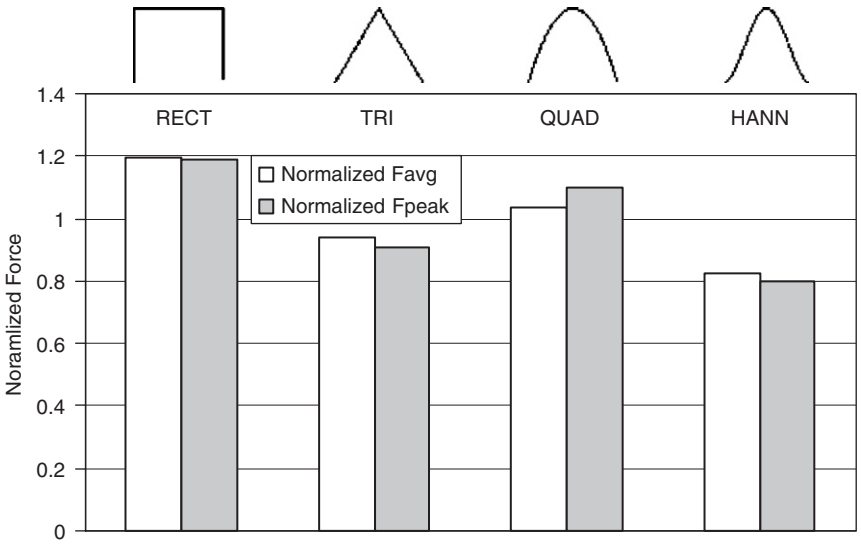

Fig. 9. Normalized average (unfilled bars) and peak (filled bars) muscle forces from the simulations using the four excitation waveforms for the pedaling task (RECT = rectangular, TRI = triangular, QUAD = quadratic, HANN = Hanning). Forces were lower for sloped waveforms than those for the rectangular waveform.

less error than those results generated using rectangular excitation waveforms. An important finding related to the second objective was that rectangular excitation waveforms lead to average and peak muscle forces being overestimated.

The most important finding of our study is that forward dynamic simulations that use optimized sloped excitation waveforms more accurately track the kinematics and kinetics (Fig. 5) and the onset and offset timing of the excitation (Figs. 6 and 7) of submaximum-effort repetitive dynamic tasks than simulations using a rectangular excitation waveform. Accordingly, it is reasonable to accept that the muscle quantities computed are more accurate as well for the sloped waveforms (Table 1). The differences in the intersegmental moments, onset and offset timing, and/or muscle forces are large enough that conclusions drawn from forward dynamic simulations may differ depending on the excitation waveform used.

Four potentially competing factors in developing a forward dynamic model are accuracy, the ability to verify input parameters, applicability, and the amount of resources to implement the model. Two of the three control parameters (onset and offset time) defining rectangular excitation waveforms can be verified by comparing these values to EMG data (Piazza and Delp, 1996; Raasch et al., 1997; Neptune and Hull, 1998). However, accuracy may be compromised if the simulated excitation waveform does not replicate important features of the actual excitation. More complex simulated excitation waveforms (i.e. increased number of control parameters) have been derived from piecewise-continuous multinodal excitation signals (Anderson and Pandy, 2003; Thelen et al., 2003). Because a greater number of control parameters will allow for a larger range of simulated kinetic and kinematic frequencies, accuracy is expected to improve when performing a tracking problem. However, verification becomes difficult when individual control parameters are not measurable. The parameters defining EMG driven models may be calibrated for high simulation accuracy (Lloyd and Besier, 2003) and EMG-driven models may provide insight into the effects of different excitation patterns on the same task. However, these models cannot be applied to muscles in which the EMG signal is not available (e.g. deep muscles and muscles simulated in open-ended optimization problems) and additional resources must be used to calibrate the model. While each waveform method has its advantages, sloped excitation waveforms provide a balance in accuracy (they are more accurate than rectangular waveforms), verification (a greater percentage of the control parameters can be verified than in static optimization methods), application (they can be used in both tracking and open-ended simulations), and resources (no calibrating experiments are required).

The analyses of the elbow-extension and pedaling simulations complemented each other. The single-degree-of-freedom elbow extension task provided greater experimental control and required a simpler model with fewer potential sources of error and variability. Pedaling represented a more complex activity with which to test the hypothesis that sloped waveforms generate more accurate simulations than rectangular waveforms. While the sloped waveforms did generate smaller tracking errors than a rectangular waveform (from 1% to 6%), these differences were not as large as those in the elbow extension simulations (from 16% to 26%, Table 1).

The smaller differences in tracking errors when using sloped excitation waveforms for the pedaling task than the elbow extension task were likely due more to the complexity of the task and the attendant model than the ability of sloped excitation waveforms to accurately model the neural excitation. Whereas a single burst, or phase, of activity was demonstrated for the elbow extension tasks, some of the muscles during pedaling have more than one burst, or multiphasic excitation (Hakansson and Hull, 2005). However, multiphasic EMG is demonstrated only in the muscles crossing the ankle. These muscles contribute relatively little of the total work during a crank cycle (Raasch et al.,1997), so that using multiphasic excitation waveforms for these muscles in simulation trials did not improve simulation results. However, in other tasks where the excitation is multiphasic and the work of the muscles is substantial, the use of multiphasic waveforms may be advantageous. Multiphasic waveforms can be easily constructed by using a summation of two (or more) of the sloped excitation waveforms presented herein.

While many different sloped excitation waveforms could have been used in this study, the three used were chosen for specific reasons. Most important was that all three were defined by the same number of parameters (3) as a rectangular waveform. Optimizing a greater number of parameters would inherently generate smaller tracking errors and thus would introduce a confounding variable. The triangular waveform represented, in a sense, the opposite of a rectangular waveform in that the slope of a triangular waveform is as small as possible. The Hanning waveform, with a first-derivative continuous throughout the cycle, represented the continuous nature of muscle recruitment. Finally, the quadratic waveform represented a slope in between those of the rectangular and triangular.

In the comparison of elbow extension simulation results for the various waveforms, the effects of errors generated from inaccurate estimates of physiological cross-sectional areas, muscle rest length (as defined in Zajac, 1989), pennation angle, shape of the length-tension relationship were minimized because the same model was used in all simulations within a subject. Consequently, any error would be present as a comparable bias in all simulations within a subject. Thus this bias had minimal effects on the results because the analyses considered differences between the simulation results within a subject.

In summary, cyclic elbow extension and pedaling tasks provided an effective means by which to validate the use of sloped excitation waveforms in forward dynamic simulations. Sloped excitation waveforms better replicate the EMG onset and offset timing and, when used in forward dynamic simulations, generate more accurate tracking than a rectangular waveform. Simulations using rectangular waveforms may overestimate the actual muscle forces. The use of sloped excitation waveforms increases the accuracy of, and confidence in, results from forward dynamic simulations.

Acknowledgments

This work was supported in part by the National Institute for Disability Related Research (NIDRR) (Award Number H133G0200137). We thank the Western Human Nutrition Research Center for the use of the Cybex 6000 ergometer.

References

Anderson, F.C., Pandy, M.G., 2003. Individual muscle contributions to support in normal walking. Gait Posture 17, 159–169.

Bedingham, W., Tatton, W.G., 1984. Dependence of EMG responses evoked by imposed wrist displacements on pre-existing activity in the stretched muscles. Canadian Journal of Neurological Sciences 11, 272–280.

Bobbert, M.F., van Zandwijk, J.P., 1999. Sensitivity of vertical jumping performance to changes in muscle stimulation onset times: a simulation study. Biological Cybernetics 81, 101–108.

Camilleri, M.J., Hull, M.L., 2005. Are maximum shortening velocity and the shape parameter in a Hill-type equation of whole muscle related to activation? Journal of Biomechanics 38, 2172–2180.

de Leva, P., 1996. Adjustments to Zatsiorsky-Seluyanov's segment inertia parameters. Journal of Biomechanics 29, 1223–1230.

Delagi, E.F., Perotto, A., 1980. Anatomic Guide for the Electromyographer–the Limbs. Thomas, Springfield, IL.

Goffe, W.L., Ferrier, G.D., Rogers, J., 1994. Global optimization of statistical functions with simulated annealing. Journal of Econometrics 60, 65–99.

Hakansson, N.A., Hull, M.L., 2005. Functional role of the leg muscles when pedaling in the recumbent versus the upright position. Journal of Biomechanical Engineering 127, 301–310.

Li, G., Kawamura, K., Barrance, P., Chao, E.Y., Kaufman, K., 1998. Prediction of muscle recruitment and its effect on joint reaction forces during knee exercises. Annals of Biomedical Engineering 26, 725–733.

Lloyd, D.G., Besier, T.F., 2003. An EMG-driven musculoskeletal model to estimate muscle forces and knee joint moments in vivo. Journal of Biomechanics 36, 765–776.

Neptune, R.R., Hull, M.L., 1998. Evaluation of performance criteria for simulation of submaximal steady-state cycling using a forward dynamic model. Journal of Biomechanical Engineering 120, 334–341.

Newmiller, J., Hull, M.L., Zajac, F.E., 1988. A mechanically decoupled two force component bicycle pedal dynamometer. Journal of Biomechanics 21, 375–386.

Piazza, S.J., Delp, S.L., 1996. The influence of muscles on knee flexion during the swing phase of gait. Journal of Biomechanics 29, 723–733.

Raasch, C.C., Zajac, F.E., Ma, B., Levine, W.S., 1997. Muscle coordination of maximum-speed pedaling. Journal of Biomechanics 30, 595–602.

Thelen, D.G., Anderson, F.C., Delp, S.L., 2003. Generating dynamic simulations of movement using computed muscle control. Journal of Biomechanics 36, 321–328.

Zajac, F.E., 1989. Muscle and tendon: properties, models, scaling, and application to biomechanics and motor control. Critical Reviews in Biomedical Engineering 17, 359–411.